Short Papers

Minimal Surfaces Based Object Segmentation

Vincent Caselles, Ron Kimmel,
Guillermo Sapiro, *Member, IEEE*, and Catalina Sbert

Abstract—A geometric approach for 3D object segmentation and representation is presented. The segmentation is obtained by deformable surfaces moving towards the objects to be detected in the 3D image. The model is based on curvature motion and the computation of surfaces with minimal areas, better known as *minimal surfaces*. The space where the surfaces are computed is induced from the 3D image (volumetric data) in which the objects are to be detected. The model links between classical deformable surfaces obtained via energy minimization, and intrinsic ones derived from curvature based flows. The new approach is stable, robust, and automatically handles changes in the surface topology during the deformation.

Index Terms—3D segmentation, minimal surfaces, deformable models, mean curvature motion, medical images.

———————————— ✦ ————————————

1 INTRODUCTION

ONE of the basic problems in image analysis is object detection. It can be associated with the problem of boundary detection, when boundaries are defined as curves or surfaces separating homogeneous regions. "Snakes," or active contours, were proposed by Kass et al. in [16] to solve this problem, and were later extended to 3D surfaces. The classical snakes and 3D deformable surfaces approach are based on deforming an initial contour or surface towards the boundary of the object to be detected. The deformation is obtained by minimizing a functional designed so that its (local) minima is at the boundary of the object [3], [33]. The energy usually involves two terms, one that controls the smoothness of the surface and the other that attracts it to the object's boundary. The topology of the final surface is, in general, as that of the initial one, unless special procedures are used to detect possible splitting and merging [23], [30]. This approach is also nonintrinsic, i.e., the energy functional depends on the parameterization. See, for example, [22], [36] for comments on advantages and disadvantages of such energy approaches for deforming surfaces.

Intrinsic models[1] of deformable contours/surfaces were simultaneously proposed by Caselles et al. [4] and by Malladi et al. [22]. In these models, the curve/surface is propagating by an implicit velocity that also contains two terms, one related to the regularity of the deforming shape and the other that attracts it to

——————————————

- *V. Caselles and C. Sbert are with the Department of Mathematics and Information, University of Illes Balears, 07071 Palma de Mallorca, Spain.*
  E-mail: dmivca0@ps.uib.es.
- *R. Kimmel is with the Lawrence Berkeley Laboratory, Mail-stop 50A-2152, University of California, Berkeley, Berkeley, CA 94720.*
  E-mail: ron@math.lbl.gov.
- *G. Sapiro is with Hewlett-Packard Labs, 1501 Page Mill Road, Palo Alto, CA 94304. E-mail: guille@hpl.hp.com.*

the boundary. This model is given by a geometric deformation flow (PDE), based on mean curvature motion, and originally was not presented as the result of minimizing an energy functional.[2] Unlike the original snakes models, the ones in [4], [22] are completely geometric (intrinsic), and do not depend on the parametrization of the evolving curve/surface.[3] This model automatically handles changes in topology when implemented using the level-sets numerical algorithm [25].

In [5], we have shown the formal mathematical relation between these two approaches for 2D object detection. We have also presented an extension and introduced the *geodesic active contours*. The geodesic active contours consider the object boundaries as geodesics in a Riemannian space whose metric is derived from the image. It has the following main properties:

1) It connects, in a formal mathematical way and for the first time, energy [16], [33] and curve evolution approaches [4], [22] of active contours.
2) It presents the snake problem as a geodesic computation one.
3) It improves existing models as a result of the geodesic formulation. This is due to the fact that the formal connection between intrinsic and classical snakes benefits from the advantages of both: The geometric and topology independent form of the models in [4], [22], combined with the important attraction forces in classical snakes that results from minimizing a meaningful functional. These forces allow, for example, the robust detection of objects with high variation in their boundary gradient. This task was impossible to achieve with the models in [4], [22] (an example for this is given later in this paper).
4) It holds formal existence, uniqueness, and stability results (which also hold for the models in [4], [22]).
5) It stops automatically, and the segmented object is obtained as the steady state of the flow.

In this paper we extend the results in [5] to 3D object detection. The metric for the 2D geodesic active contours is extended to 3D. The resulting flow is based on geometric deformable *surfaces*. This flow has advantages over other 3D deformable models similar to the advantages of the geodesic active contours over previous 2D approaches. We show that the desired boundary is given by a "minimal surface," or a surface of "minimal weighted area."

Our 3D model is related to a number of previously or simultaneously developed results. It is of course closely related to the works of Terzopoulos and colleagues on energy based deformable surfaces, as well as to the works in [4], [22]. The similitude and differences with those approaches and the recent ones in [17], [29], [31], [34], will be presented after describing the basic principles of the different models.

————————————

1. We use the term "intrinsic" for these models since they are based on intrinsic differential geometry.

2. As was shown in [5], [17] for the 2D active contours case and will be presented later in this paper for the 3D ones, a term is missing in these intrinsic models to be a complete gradient-descent flow.

3. Dependency on the parametrization means that different representations/parametrizations of the evolving surface may yield different results.

2 BASIC APPROACHES TO DEFORMABLE MODELS

2.1 Energy Based Models

The 3D extension of the basic 2D snakes, known as the deformable surface model, was introduced by Terzopoulos et al. [33]. It was improved and applied by many others (e.g., [9], [10], [32]). In the 3D case, a parameterized surface $v(r, s) = (x(r, s), y(r, s), z(r, s))$, $(r, s) \in [0, 1] \times [0, 1]$, is considered, and the energy functional is given by

$$E(v) = \int_\Omega \left[\omega_{10} \left| \frac{\partial v}{\partial r} \right|^2 + \omega_{01} \left| \frac{\partial v}{\partial s} \right|^2 + \omega_{11} \left| \frac{\partial^2 v}{\partial r \partial s} \right|^2 + \omega_{20} \left| \frac{\partial^2 v}{\partial r^2} \right|^2 + \omega_{02} \left| \frac{\partial^2 v}{\partial s^2} \right|^2 + P \right] dr ds$$

where $P := -\|\nabla I\|^2$, or any related decreasing function of the gradient, I is the 3D image where objects are to be detected, and ω_{ij} are given constants (model parameters). The first terms of $E(v)$ are related to the smoothness of the surface, while the last term relates to the attraction of the surface to the object. The algorithm starts with an initial surface S_0, generally near the desired 3D boundary O, and tries to move S_0 towards a local minimum of E. The idea is that the surface is attracted to the object via P, while the smoothness constrains are dictated by the first terms in $E(v)$. Note that $E(v)$ depends on the surface parametrization.

2.2 Intrinsic Models

The 3D intrinsic deformable models for segmentation [4], [22] consider surfaces that smoothly move towards the objects in the image. These models are parametrization independent, that is, the moving forces depend on intrinsic geometric characteristics of the image and the evolving surface.

Let $Q =: [0, a] \times [0, b] \times [0, c]$ and $I : Q \to \mathbb{R}^+$ be a given 3D data image. Let $g(I) := 1 / \left(1 + \left| \nabla \hat{I} \right|^p \right)$, where $\hat{I}$, a regularized version of I, and $p = 1$ or 2. $g(I)$ acts as an edge detector so that the object we are looking for is ideally given by the equation $g = 0$. Our initial active surface S_0 will be embedded as a level set [25] of a function $u_0 : Q \to \mathbb{R}^+$, say $S_0 = \{x : u_0(x) = 0\}$, with u_0 being positive in the exterior and negative in the interior of S_0. The evolving active surface is defined by $S(t) = \{x : u(t, x) = 0\}$ where $u(t, x)$ is the solution of

$$\frac{\partial u}{\partial t} = g(I)|\nabla u|\text{div}\left(\frac{\nabla u}{|\nabla u|} \right) + vg(I)|\nabla u| = g(I)(v + \mathbf{H})|\nabla u|, \quad (1)$$

with initial condition $u(0, x) = u_0(x)$ and Neumann boundary conditions. Here $\mathbf{H} = \text{div}\left(\frac{\nabla u}{|\nabla u|} \right)$ is the sum of the two principal curvatures of the level sets S (twice its mean curvature,) and v is a positive real constant. The sign conventions are adopted to obtain inwards propagating surfaces. For surfaces evolving from the inside outwards, we take $v < 0$. This is a drawback of this model: The surfaces prefer to propagate in the curvature direction (see, e.g., [31]).

This model was heuristically justified in [4], [22]. It can be described as the composition of:

1) A smoothing term: Twice the mean curvature in the case of (1). More efficient smoothing velocities as those proposed in [2], [7], [24] can be used instead of $\mathbf{H}$.[4] Note again that unlike classical energy based models, this component of the deforming surface is intrinsic.

2) A constant balloon-type force ($v|\nabla u|$). Similar to the energy based models, this term is necessary in this case for the detection of nonconvex objects.

3) A stopping factor ($g(I)$). Note that the energy models have an attraction term, obtained from P in $E(v)$, and not a stopping term as (1). The geodesic and minimal surfaces models improve those approaches.

3 DEFORMABLE MODELS AS MINIMAL SURFACES

In [5], a model for 2D object detection based on the computation of geodesics in a given Riemannian space was presented. This means that we compute paths or curves of minimal (weighted) length. We showed, based on classical principles of dynamical systems, that both energy-based and curve-evolution-based models are mathematically related to the minimization of a weighted length of the form $\int g(I) \, ds$, where $g(I)$ is a decreasing function of the image gradient as before and s is the Euclidean arc-length. This idea can be extended to 3D. In this case, length is replaced by surface area $A := \int \int da$, and weighted length by "weighted area"

$$A_R := \int \int g(I) \, da$$

where da is the (Euclidean) element of area. Surfaces minimizing A are called *minimal surfaces* [26]. In the same manner, we will denote by minimal surfaces those surfaces that minimize A_R. The area element da is given by the classical area element in Euclidean space, while the "area element" da_r is given by $g(I) \, da$. The basic element of our deformable model will be given by minimizing A_R by means of an evolution equation obtained from its Euler-Lagrange. Let us point out the basic characteristics of this flow.

The Euler-Lagrange of A is given by the mean curvature $\mathbf{H}$, that results in the curvature (steepest descent) flow $\frac{\partial S}{\partial t} = \mathbf{H}\bar{\mathcal{N}}$, where S is the 3D surface and $\bar{\mathcal{N}}$ its inner unit normal. With the sign conventions explained above, the corresponding level set [25] formulation is

$$u_t = |\nabla u|\text{div}\left(\frac{\nabla u}{|\nabla u|} \right) = |\nabla u|\mathbf{H}$$

Therefore, the mean curvature motion provides a flow that computes (local) minimal surfaces [8]. The Euler-Lagrange of A_R, yields the flow

$$\frac{\partial S}{\partial t} = \left(g\mathbf{H} - \nabla g \cdot \bar{\mathcal{N}} \right)\bar{\mathcal{N}} \qquad (2)$$

This is the basic weighted minimal surface flow. Using the level sets representation, the steepest descent method to minimize A_R yields

$$\frac{\partial u}{\partial t} = |\nabla u|\text{div}\left(g(I) \frac{\nabla u}{|\nabla u|} \right) = g(I)|\nabla u|\text{div}\left(\frac{\nabla u}{|\nabla u|} \right) + \nabla g(I) \cdot \nabla u \qquad (3)$$

We note that unlike previous intrinsic surface evolution approaches for 3D object detection [4], [22], the minimal surfaces model includes a new term, $\nabla g \cdot \nabla u$. This term is fundamental for detecting boundaries with fluctuations in their gradient, task that was not possible with the model (1); see Fig. 3 and [5] for details.

As in the 2D case, we can add a constant force to the minimization problem (minimizing the weighted volume $\int g \, dx \, dy \, dz$), obtaining the general *minimal surfaces model* for object detection:

$$\frac{\partial u}{\partial t} = |\nabla u|\text{div}\left(g(I) \frac{\nabla u}{|\nabla u|} \right) + vg(I)|\nabla u| \qquad (4)$$

This is the flow we will further analyze and use for 3D object detection. It has the same properties and geometric characteristics as the geodesic active contours, leading to accurate numerical implementations and topology-free object segmentation. Furthermore, the following results can be proved for this flow:

---

4. Although curvature flows smooth 2D curves [14], [15], [28], a 3D geometric flow that smoothes all possible surfaces was not found [24]. Frequently used are mean curvature or the positive part of the Gaussian curvature flows [2], [7].

THEOREM 1. ([6]) *Assume that $g \geq 0$ is sufficiently smooth. Then, for any Lipschitz initial condition u_0, there exists a unique viscosity solution $u(t, x)$ of (4) with $u(0, x) = u_0(x)$.*

In practice, we choose an initial condition u_0 with $\{x : u_0(x) \leq 0\}$ containing the desired object and we let it evolve according to (4). The active surface $S(t)$ is the boundary of the set $\{x : u(t, x) \leq 0\}$. One can show [6] the independence of the evolution from the particular function u_0 used to define the initial active surface. Finally, the model (4) enables us to show the correctness of the geometric formulation in some special yet important cases. We have:

THEOREM 2. ([6]) *Assume that $S = \{x : g(x) = 0\}$ is a compact connected smooth surface embedded in $\mathbb{R}^3$, which is unknotted. Then, if the constant v is sufficiently large, then $S(t) \to S$ in the Hausdorff distance as $t \to \infty$. The same result can be proved for all compact smooth surfaces which can be unknotted by adding to them a finite number of handles, and also for finite unions of surfaces in that class.*

Theorem 2 shows the consistency of the model and covers a large class of surfaces which can be found in practice. Several issues arise concerning this theorem:

1) How large should the constant v be? It can be seen from the proof in [6] that v should be larger than the mean curvature of the evolving surfaces. A reasonable assumption is that v should be larger than the curvature of the desired surface. On the other hand, for initial condition of a surface close to the desired object, one can choose $v = 0$. In practice, convergence can also be obtained for $v = 0$ if obstacles do not stop the active surface, yet the process is slower.

2) The presence of noise may disturb the convergence. This can be avoided by preprocessing the original image I. In practice, if the noise is not dominant and is not structured along a surface, it will not stop the active surface.

3) The above theorem assumes that the desired surface is given by $g(x) = 0$. In [6], we give the proof for this case, as stated in the above theorem. Note that even if $g > 0$, the solution to the flow exists, is unique, and arrives to a steady state. If $g(x) > 0$ along the desired surface, the equilibrium position will be along the local minimum and a balance of the forces yields the result. This is one of the cases where the new force $\nabla g \cdot \nabla u$ plays an important role (previous intrinsic models do not have a steady state if $g \neq 0$). The determination of the exact point of equilibrium for a given description of the image is the subject of further research.

In [12] it was shown that the curvature along the 2D geodesics minimizing the weighted arclength may be bounded by

$$|\kappa| \leq \sup_{p \in [0,a] \times [0,b]} \left\{ \frac{|\nabla g(I(p))|}{g(I(p))} \right\}$$

It is easy to see that there is no need for the geodesic itself for limiting the curvature values. In [12], motivated by [20], this bound helped in the construction of different potential functions.

A straightforward generalization of this result to our three dimensional model yields the bound over the mean curvature $\mathbf{H}$. From the equations above, it is clear that at steady state (i.e., $S_t = 0$), the mean curvature along the surface S is given by

$$H = \frac{\nabla g \cdot \vec{\mathcal{N}}}{g} - v$$

We readily obtain the following upper bound for the mean curvature magnitude along the final surface

$$|\mathbf{H}| \leq \sup \left\{ \frac{|\nabla g|}{g} \right\} + |v|$$

where the sup operation is taken over all the 3D domain. The above bound gives an estimation of the allowed gaps in the edges of the object to be detected as a function of v. A pure gap is defined as a part of the object boundary at which, for some reason, $g = \text{constant} \neq 0$ in a large enough neighborhood. At these locations $|\mathbf{H}| = |v|$. Therefore, pure gaps of radius larger than $1/v$ will cause the propagating surface to penetrate into the segmented object. It is also clear that $v = 0$ allows the detection of gaps of any given size, and the boundary at such places will be detected as the minimal surface "gluing" the gaps boundaries.

The basic equations for 3D segmentation here described, and those for 2D in [5], were recently independently proposed in [17], [18], [35] based on a slightly different initial approach. Shah [29] also recently presented a 2D active contours formulation as the one in [5], which is the 2D analogue of the model here described. Although these works also present the problem of 2D active contours as geodesic computations, they do not show the formal connections between classical energy models and curve evolution ones. Actually, to the best of our knowledge, none of the previous works on curve/surface evolution for object segmentation show the mathematical relation between those models and classical energy approaches. Actually, in general the two approaches are considered independent. Although the extension from the 2D model to the 3D one is easy, no 3D examples are presented in [17], [18], [29]. Also, not all the theoretical results here quoted [6] can be found in [17], [18], [29] (in [18] the authors do show a number of very important theoretical results as those in [6] and quoted here, as well as the 3D formulation). Three-dimensional examples are given in [34], where similar equations are proposed. The equations there are obtained by extending the flows in [4], [22], again without showing that they can be obtained in a natural fashion from a reinterpretation of energy-based formulations via minimal surfaces. In [31], the authors based their work on the models in [4], [22]. One of the key ideas there, motivated by the shape theory of shocks developed in [19], is to perform multiple initializations. A normalized version of A was derived in [13] from a different point of view, giving as well different flows for 2D active contours. Extension of that model to 3D was presented in [11].

4 EXPERIMENTAL RESULTS

We now present some examples of our minimal surfaces deformable model (4). The numerical implementation is based on the algorithm for surface evolution via level sets [25]. It allows the evolving surface to change topology without monitoring the deformation. Using new results in [1], the algorithm can be very efficient. In the numerical implementation of (4) we have chosen central difference approximation in space and forward difference approximation in time. This simple selection is possible due to the
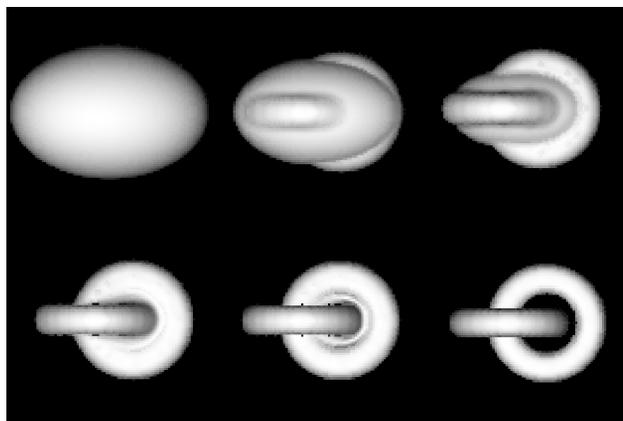
Fig. 1. Detection of two linked tori.
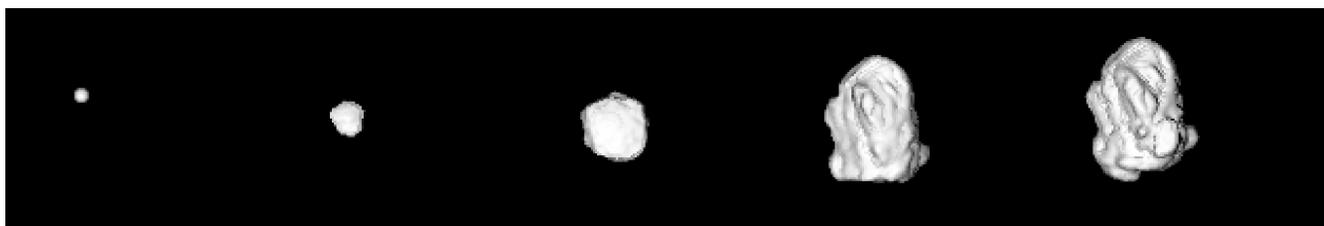
Fig. 2. Detection of a tumor in MRI.
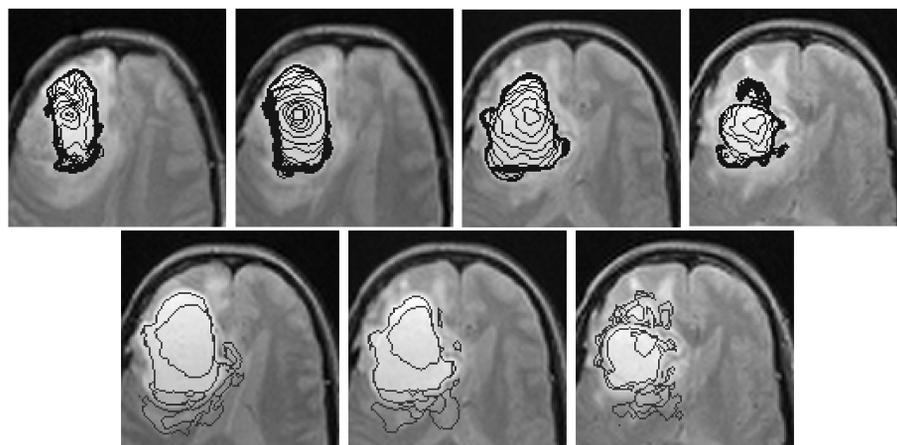
Fig. 3. Slices of the 3D detection in Fig. 2, with the proposed model (top) and the previous models (bottom). This figure shows the importance of the new gradient term. Without that term, the model fails to stop and continues to evolve as shown.
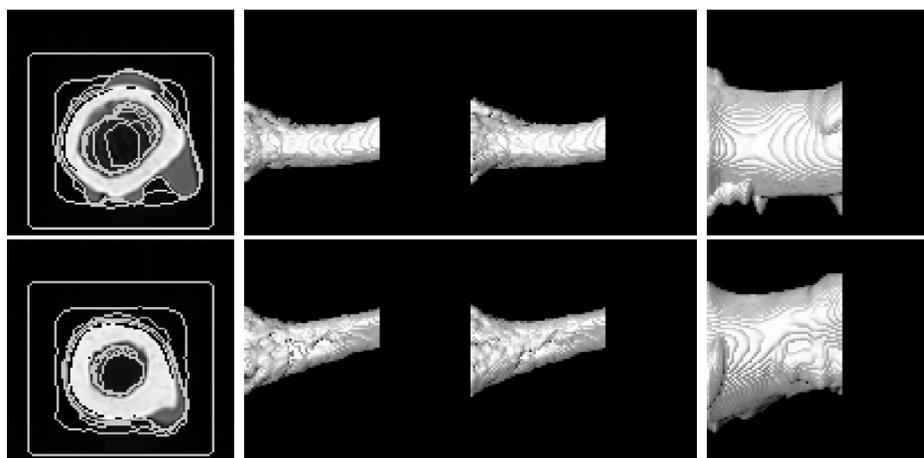
Fig. 4. Two slices and two orthographic views of 3D detection of the inner and outer parts of a bone in an MRI image.

stable nature of the equation, however, when the coefficient v is taken to be of high value or when the gradient term is dominant, more sophisticated approximations are required [25].

The first example of the minimal surfaces deformable model is presented in Fig. 1. A "knotted surface" composed of two tori forming a "chain" is detected. The initial surface is an ellipsoid surrounding the two tori (top left). Note how the model manages to change its topology and detect the final surface (bottom right).

Fig. 2 presents the 3D detection of a tumor in an MRI image. The initial surface is presented on the left followed by three evolution steps. The final surface, the "weighted minimal surface," is presented on the right. Fig. 3 (top) shows four slices of the 3D evolving surface painted on the corresponding MRI data. Slices of the initial surface are represented by the smallest curves inside the tumor. The outer contours are the detected object, and are obtained as the steady-state of the flow. The contours in between represent

stages of the evolving surface. When we applied the model without the new gradient term ($\nabla g \cdot \nabla u$) on the same MRI data, the propagating surface did not stop at the boundary. This is shown in Fig. 3, bottom, where the contours propagate outside of the tumor area (see for example bottom part of the slices, where the contours exit the tumor area).

Fig. 4 presents the segmentation of the interior and exterior of a 3D MRI data of a bone. The two slices show the process of locating the outer and inner parts (left). The initial surfaces are represented by the small curve inside the bone and the square outside it (these are slices of the initial surface). The other curves represent slices of the evolving surface. Two views of the final segmentation of the inner (middle) and outer (right) parts are presented in upper and lower rows.

5 CONCLUDING REMARKS

In this paper we presented a novel formulation of deformable surfaces for 3D object detection, extending our previous 2D work [5]. The object is given as a "minimal surface." This means that detecting the object is equivalent to finding a surface of minimal "weighted area," where the weight is given by the image. The minimal surfaces formulation introduced a new term that attracts the deforming surface to the boundary, improving the detection of boundaries with large variations in their gradient. This new term also frees the model from the need to estimate critical parameters. Therefore, the minimal surfaces formulation not only connects previous models, but also improves them. Results regarding existence, uniqueness, stability, and correctness of the solution obtained by our model were summarized and will be reported elsewhere.

Experiments for different kind of images were presented. These experiments demonstrate the ability to detect several objects, as well as the power to simultaneously detect interior and exterior boundaries. The subpixel accuracy intrinsic to the algorithm allows us to perform accurate measurements after the object is detected [21], [27].

REFERENCES

[1] D. Adalsteinsson and J.A. Sethian, "A Fast Level Set Method for Propagating Interfaces," *J. Comparative Physics*, vol. 118, pp. 269–277, 1995.

[2] L. Alvarez, F. Guichard, P.L. Lions, and J.M. Morel, "Axioms and Fundamental Equations of Image Processing," *Architecture Rational Mechanics*, vol. 123, 1993.

[3] A. Blake and A. Zisserman, *Visual Reconstruction*. Cambridge, Mass.: MIT Press, 1987.

[4] V. Caselles, F. Catte, T. Coll, and F. Dibos, "A Geometric Model for Active Contours," *Numerische Mathematik*, vol. 66, pp. 1–31, 1993.

[5] V. Caselles, R. Kimmel, and G. Sapiro, "Geodesic Active Contours," *Int'l J. Computer Vision*, forthcoming. A short version appears in *Proc. ICCV '95*, pp. 694–699, Cambridge, June 1995.

[6] V. Caselles, R. Kimmel, G. Sapiro, and C. Sbert, "Minimal Surfaces: A Three-Dimensional Segmentation Approach," Technion Technical Report 973, June 1995, Israel.

[7] V. Caselles and C. Sbert, "What Is the Best Causal Scale-Space for 3D Images?," *SIAM J. Applied Math*, forthcoming.

[8] D. Chopp, "Computing Minimal Surfaces via Level Set Curvature Flows," *J. Comparative Physics*, vol. 106, no. 1, pp. 77–91, 1993.

[9] L.D. Cohen, "On Active Contour Models and Balloons," *CVGIP: Image Understanding*, vol. 53, pp. 211–218, 1991.

[10] I. Cohen, L.D. Cohen, and N. Ayache, "Using Deformable Surfaces to Segment 3D Images and Infer Differential Structure," *CVGIP: Image Understanding*, vol. 56, pp. 242–263, 1992.

[11] L.D. Cohen and I. Cohen, "Finite Element Methods for Active Contour Models and Balloons for 2D and 3D Images," *IEEE Trans. Pattern Analysis and Machine Intelligence*, vol. 15, pp. 1,131–1,147, 1993.

[12] L.D. Cohen, and R. Kimmel, "Global Minimum for Active Contours Models: A Minimal Path Approach," *Int'l J. Computer Vision*, forthcoming. A short version appears in *Proc. CVPR '96*, San-Francisco, Calif., 1996.

[13] P. Fua and Y.G. Leclerc, "Model Driven Edge Detection," *Machine Vision and Applications*, vol. 3, pp. 45–56, 1990.

[14] M. Gage and R.S. Hamilton, "The Heat Equation Shrinking Convex Plane Curves," *J. Differential Geometry*, vol. 23, pp. 69–96, 1986.

[15] M. Grayson, "The Heat Equation Shrinks Embedded Plane Curves to Round Points," *J. Differential Geometry*, vol. 26, pp. 285–314, 1987.

[16] M. Kass, A. Witkin, and D. Terzopoulos, "Snakes: Active Contour Models," *Int'l J. Computer Vision*, vol. 1, pp. 321–331, 1988.

[17] S. Kichenassamy, A. Kumar, P. Olver, A. Tannenbaum, and A. Yezzi, "Gradient Flows and Geometric Active Contour Models," *Proc. ICCV '95*, pp. 810–815, Cambridge, June 1995.

[18] S. Kichenassamy, A. Kumar, P. Olver, A. Tannenbaum, and A. Yezzi, "Conformal Curvature Flows: From Phase Transitions to Active Vision," *Archive for Rational Mechanics and Analysis*, forthcoming.

[19] B.B. Kimia, A. Tannenbaum, and S.W. Zucker, "Shapes, Shocks, and Deformations, I," *Int'l J. Computer Vision*, vol. 15, pp. 189–224, 1995.

[20] R. Kimmel, A. Amir, A.M. Bruckstein, "Finding Shortest Paths on Surfaces Using Level Sets Propagation," *IEEE Trans. Pattern Analysis and Machine Intelligence*, vol. 17, no. 6, pp. 635–640, June 1995.

[21] R. Malladi, R. Kimmel, D. Adalsteinsson, G. Sapiro, V. Caselles, and J.A. Sethian, "A Geometric Approach to Segmentation and Analysis of 3D Medical Images," *Proc. Math. Methods Biomedical Image Analysis Workshop*, San Francisco, June 21–22, 1996.

[22] R. Malladi, J.A. Sethian, and B.C. Vemuri, "Shape Modeling with Front Propagation: A Level Set Approach," *IEEE Trans. Pattern Analysis and Machine Intelligence*, vol. 17, no. 2, pp. 158–175, Feb. 1995.

[23] T. McInerney and D. Terzopoulos, "Topologically Adaptable Snakes," *Proc. ICCV '95*, pp. 840–845, Cambridge, June 1995.

[24] P.J. Olver, G. Sapiro, and A. Tannenbaum, "Invariant Geometric Evolutions of Surfaces and Volumetric Smoothing," *SIAM J. Applied Math.*, forthcoming.

[25] S.J. Osher and J.A. Sethian, "Fronts Propagation with Curvature Dependent Speed: Algorithms Based on Hamilton-Jacobi Formulations," *J. Computational Physics*, vol. 79, pp. 12–49, 1988.

[26] R. Osserman, *Survey of Minimal Surfaces*. Dover, 1986.

[27] G. Sapiro, R. Kimmel, and V. Caselles, "Object Detection and Measurements in Medical Images via Geodesic Active Contours," *Proc. SPIE-Vision Geometry*, San Diego, July 1995.

[28] G. Sapiro and A. Tannenbaum, "Affine Invariant Scale-Space," *Int'l J. Computer Vision*, vol. 11, no. 1, pp. 25–44, 1993.

[29] J. Shah, "Recovery of Shapes by Evolution of Zero-Crossings," technical report, Math. Dept., Northeastern Univ., Boston, Mass., 1995.

[30] R. Szeliski, D. Tonnesen, and D. Terzopoulos, "Modeling Surfaces of Arbitrary Topology with Dynamic Particles," *Proc. CVPR*, pp. 82–87, 1993.

[31] H. Tek and B.B. Kimia, "Image Segmentation by Reaction-Diffusion Bubbles," *Proc. ICCV '95*, pp. 156–162, Cambridge, June 1995.

[32] D. Terzopoulos and D. Metaxas, "Dynamic 3D Models with Local and Global Deformations: Deformable Superquadrics," *IEEE Trans. Pattern Analysis and Machine Intelligence*, vol. 13, pp. 703–714, 1991.

[33] D. Terzopoulos, A. Witkin, and M. Kass, "Constraints on Deformable Models: Recovering 3D Shape and Nonrigid Motions," *Artificial Intelligence*, vol. 36, pp. 91–123, 1988.

[34] R.T. Whitaker, "Algorithms for Implicit Deformable Models," *Proc. ICCV '95*, pp. 822–827, Cambridge, June 1995.

[35] A. Yezzi, S. Kichenassamy, P. Olver, and A. Tannenbaum, "A Geometric Snake Model for Segmentation of Medical Imagery," *IEEE Trans. Medical Imaging*, forthcoming.

[36] S.C. Zhu, T.S. Lee, and A.L. Yuille, "Region Competition: Unifying Snakes, Region Growing, Energy/Bayes/MDL for Multi-Band Image Segmentation," *Proc. ICCV '95*, pp. 416–423, Cambridge, June 1995.